Phase Transitions and Microstructural Changes During Oxidation and Reduction of a Weathered Ilmenite Concentrate

Hossein Salehi[1] · Stian Seim[2] · Leiv Kolbeinsen[1] · Jafar Safarian[1]

Abstract

The present work aims to investigate the link between the oxidation and reduction of a weathered ilmenite concentrate in terms of phase transitions, microstructural changes, and element distribution. An ilmenite concentrate sample was pelletized and fired at 1000 °C in air, and as a result, the pellets were oxidized. The oxidized pellets were reduced by hydrogen gas at 1000 °C, which yielded almost complete metallization of the iron content of the pellets. The ore and the pellets were characterized in each step by XRD and SEM techniques, and distribution of elements and phases were investigated. Ilmenite, pseudorutile, and rutile were the main phases detected in the ilmenite concentrate sample, and depending on the weathering degree of the particles, different fractions of the phases were identified in their microstructure. It was found that irregular rutile grains dispersed in a pseudobrookite matrix is the morphology of the oxidized ilmenite phase. However, increasing microcracks and porosities were the only microstructural changes in the pseudorutile phase after oxidation in air. Studying the specific types of the ore particles and their oxidized and reduced forms indicated that the phase distribution in the ilmenite ore particles dictates the phase distribution in the oxidized and reduced ones. Results show that the morphology of the reduced particles includes a titanium (III) oxide matrix in which reduced iron globules are dispersed.

Keywords Hydrogen · Ilmenite · Ilmenite smelting · Oxidation · Reduction · Titanium dioxide

1 Introduction

Titanium consists of about 0.6% of the earth's crust. Due to its superior corrosion resistance and strength to weight ratio, titanium has found its use in a large variety of applications, from aerospace and aeronautic industries to biomedical devices and chemical processes equipment [1]. Ilmenite is the most abundant titanium mineral and the primary starting material for titanium dioxide pigment production, which is the most widely used titanium product [2].

Today, most of the mined ilmenite is upgraded to synthetic rutile or titania-rich slag, which both are used in the pigment industry. Sulfate and chloride processes have been the main industrially used methods for producing TiO_2 pigment grade

from ilmenite [3]. However, after the Second World War, ilmenite smelting was more developed as a process in which the iron content of the ilmenite can be extracted for further utilization [4]. In this process, ilmenite, together with carbon material, is charged into an electric arc furnace, where a high titania slag forms on the top of a molten iron bath. Direct smelting of ilmenite and pre-reduction of the ore followed by a smelting step are the most conventional methods of the high titania slag process [5]. In the second method, ilmenite is usually fed into the smelter in the form of pre-reduced pellets. These pellets are produced from ground ore concentrate and are oxidized during a firing step before being reduced. The majority of previous studies on the oxidation and reduction of ilmenite have focused on process kinetics. According to the literature, the topochemical model is the best describing kinetic model for both oxidation and reduction of ilmenite [6–9]. The oxidation of ilmenite enhances the reduction kinetics due to increased porosity resulting from crystal structure changes of minerals in particles [6, 10]. Furthermore, thermodynamically, hematite in the oxidized ilmenite is more rapidly reduced than magnetite [6]. However, studies showed that impurities affect the reduction degree of ilmenite. Impurities such as magnesium oxide and manganese oxide decrease iron

✉ Hossein Salehi
hossein.salehi@ntnu.no

[1] Department of Materials Science and Engineering, Norwegian University of Science and Technology (NTNU), Trondheim, Norway

[2] TiZir Titanium and Iron, Tyssedal, Norway

activity in the oxide phase, which leads to lowering the reaction potential and slowing down the reduction rate [11, 12].

In the current work, a weathered ilmenite concentrate was pelletized, and the produced pellets were oxidized in air followed by reduction by hydrogen. Employing X-ray diffraction analysis (XRD) and scanning electron microscopy (SEM), phase transitions, microstructural changes, and elements distribution during oxidation and reduction of the pellets were studied. In most of the similar works, X-ray analysis data have been the basis for studying the phase transition of ilmenite. Studying the sequence of morphological changes during ilmenite oxidation and reduction is a new approach in which different particle types of the ore are characterized and compared with their corresponding particles after oxidation and reduction. This method provides a better understanding of the phase transition of ilmenite during both processes. It also contributes to studying the kinetics of ilmenite oxidation and reduction. The used approach improves the perception of ilmenite phase transition during smelting, as phase distribution in smelting products is dependent on the properties of the used raw materials. These data are advantageous in the calculation of energy consumption of the process.

2 Experimental Procedure

A weathered ilmenite concentrate sample in the form of powder was supplied by TiZir Titanium and Iron Company (Tyssedal, Norway). The chemical composition of the received ilmenite concentrate is given in Table 1. The average particle size of the powder is 139.2 μm, and D_{10}, D_{50}, and D_{90} are equal to 90.8 μm, 128.7 μm, and 199.6 μm, respectively.
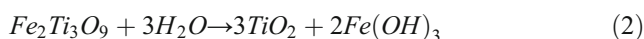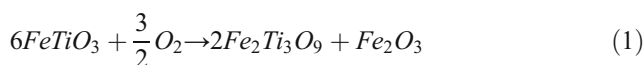
The ore microstructure was studied using a Zeiss Ultra 55 LE Field Emission Scanning Electron Microscope (FESEM) equipped with Energy-Dispersive Spectroscopy (EDS) and Back-Scattered Electron (BSE) detectors. For phase identification, a Bruker D8 A25 DaVinci™ X-ray Diffractometer (XRD) with CuKα radiation, 10–80° diffraction angle, 0.01° step size, and 60-min scanning time was employed. The ore was pelletized in a laboratory pelletizing drum to form green pellets with 3–4 mm diameter. Bentonite powder was used as the binder, and the moisture content was about 9%. The green pellets were dried overnight at 80 °C, followed by firing (oxidizing) in a muffle furnace at 1000 °C for 1 h in air. A portion of the fired pellets was reduced with hydrogen gas in a thermogravimetric furnace (DISvaDRI furnace, SINTEF) at

1000 °C for 1 h. Samples were prepared for microstructural analysis from both oxidized and reduced pellets, and they were studied by the SEM technique, as mentioned for the ore particles.

3 Results and Discussion

3.1 Phase Analysis

Figure 1 shows the XRD diffractograms of the produced oxide and reduced ilmenite pellets with the characterized phases in comparison with the raw concentrate. The ore is a weathered ilmenite deposit in which iron oxide has been partially removed by time, and therefore a portion of ilmenite has naturally altered to pseudorutile ($Fe_2Ti_3O_9$). In this phenomenon, pseudorutile is eventually altered to TiO_2 through the leaching removal of iron as hematite. The alteration pathway of ilmenite was discussed in the literature [13, 14]. The alteration occurs according to the chemical reactions represented in Eqs. 1 and 2.

$$6FeTiO_3 + \frac{3}{2}O_2 \rightarrow 2Fe_2Ti_3O_9 + Fe_2O_3 \qquad (1)$$

$$Fe_2Ti_3O_9 + 3H_2O \rightarrow 3TiO_2 + 2Fe(OH)_3 \qquad (2)$$

Pseudorutile peaks can be identified in the XRD patterns of both the concentrate and oxidized pellets. During the weathering, pseudorutile was partially formed as an intermediate phase via reaction (Eq. 1). As the alteration process goes on, based on Eq. 2, iron oxide is naturally leached out, and rutile remains as the final product. Since both of the alteration reactions (Eqs. 1 and 2) occur partially, in addition to ilmenite, pseudorutile and rutile are present in the ore [15].

Comparison of the diffraction patterns indicates that during the pellet-firing step in air, ilmenite was oxidized entirely, and pseudobrookite and hematite formed as new phases. However, it seems that the oxidation conditions did not have a significant effect on the pseudorutile phase, and it has remained one of the main phases after oxidation. Furthermore, the intensity of rutile phase peaks in the oxidized pellet is increased, which is an indication of increasing the amount of phase after the oxidation.

During the oxidation of ilmenite at temperatures higher than 800 °C, the phase transition consists of two main stages.

Table 1 Chemical analysis of the received ilmenite concentrate (wt%)

| TiO_2	Fe_2O_3	FeO	MnO	MgO	Al_2O_3	SiO_2	V_2O_5	Cr_2O_3	CaO	Zr	P_2O_5	Nb	C
54.0	23.8	18.2	1.1	0.9	0.7	0.6	0.3	0.2	0.03	0.03	0.04	0.06	0.04

Fig. 1 XRD diffractograms of (a) raw ilmenite concentrate, (b) oxidized ilmenite pellet, and (c) reduced ilmenite pellet
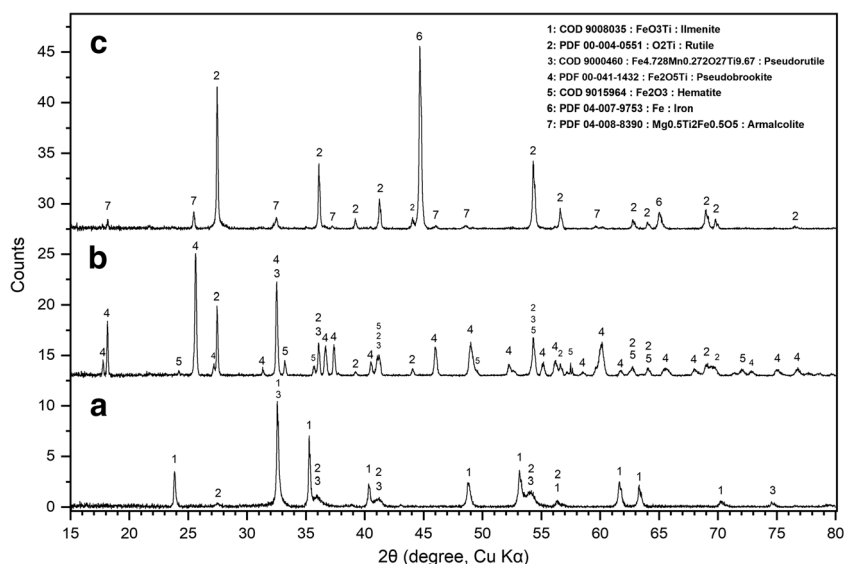

In the first stage, hematite and rutile are formed (Eq. 3). However, they react (Eq. 4) to form pseudobrookite as a thermodynamically more stable phase [16]. Therefore, the oxidation pathway of ilmenite can be summarized as follows:

$$2FeTiO_3 + \frac{1}{2}O_2 \rightarrow 2TiO_2 + Fe_2O_3 \qquad (3)$$

$$TiO_2 + Fe_2O_3 \rightarrow Fe_2TiO_5 \qquad (4)$$
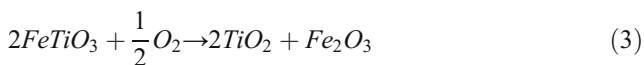
Since the reaction rate (Eq. 3) is very fast, almost all the ilmenite was oxidized. However, due to the slower reaction rate (Eq. 4) as a combination reaction [16], unreacted rutile and hematite have affected phase distribution in the oxidized ore. Comparison of the XRD diffractogram of the oxidized and reduced ore shows that the characteristic peaks of pseudorutile, pseudobrookite, and hematite disappear after the pellet is reduced, while metallic iron peaks are detected, and the intensity of the rutile peaks is increased. Equations 5 and 6 represent the reduction reactions of pre-oxidized ilmenite phase (pseudobrookite) with hydrogen [11]. In a parallel reaction, hematite content of the pre-oxidized ore is also reduced to metallic iron.

$$Fe_2TiO_5 + TiO_2 + H_2 \rightarrow 2FeTiO_3 + H_2O \qquad (5)$$

$$FeTiO_3 + H_2 \rightarrow Fe + TiO_2 + H_2O \qquad (6)$$
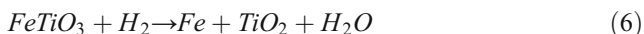
The reduction of pseudorutile with hydrogen includes ilmenite formation as an intermediate phase (Eq. 7). The ilmenite is reduced to iron and rutile afterward via reaction Eq. 6 [17].

$$Fe_2Ti_3O_9 + H_2 \rightarrow 2FeTiO_3 + TiO_2 + H_2O \qquad (7)$$
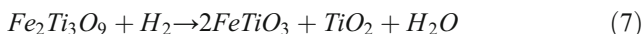
In the reduction step of the ore, Mg and Mn as the main impurities substitute for iron in the ilmenite crystal structure and not only increase the stability of the oxide phase but also form the new oxide phases. This phenomenon decreases the reactivity of Fe^{2+}, making its reduction to the metallic phase more difficult [11, 12]. Armalcolite $(Mg, Fe)Ti_2O_5$ is the new phase that was formed due to the presence of magnesium, and the manganese forms an α-oxide $(Mn, Fe, Ti)_2O_3$ [15]. However, the latter phase was not detected in the XRD analysis of the reduced ore. A simple calculation can be done to confirm the presence of armalcolite phase in the reduced ilmenite. Based on the chemical analysis of raw material, 100 g sand ilmenite contains 0.9 g MgO or 0.54 g Mg. Armalcolite with the chemical composition of $Mg_{0.5}Ti_2Fe_{0.5}O_5$ contains 6.5 wt% Mg. Considering the detection limit of the instrument is 3 to 5 wt%, there should be at least 3 to 5 g armalcolite in 100 g reduced ilmenite. The minimum amount of Mg in the armalcolite phase needed for detection based on the detection limit of 3 wt% is 0.195 g in 100 g reduced ilmenite. Therefore, there is already enough Mg to form a detectable amount of armalcolite.

3.2 Microstructural Changes Through Oxidation and Reduction

Due to partial weathering, various types of particles exist in the ore sample. These particles undergo extreme phase transformations during oxidation and reduction, as the phase analysis results above indicated. Since the diversity of the ore particles is vast, only the main ore particles were studied, and their microstructural changes in oxidation and reduction were monitored.

In Fig. 2 the Back-Scattered Electron (BSE) micrograph of different types of the main particles in the altered ilmenite ore, which are called particle types A1 to E1 here, is compared with their possible corresponding particles after oxidation (types A2–E2) and reduction (types A3–E3). Due to the difference in the atomic numbers, the Fe-rich areas are brighter

Table 2 Chemical composition of the numbered points and areas in Fig. 2 (atomic percent %)

	1	2	3	4	5	6	7	8	9	10	11	12	13	14	15	16	17	18	19	20	21	22	23
Ti	25.1	28.6	24.6	26.7	25.6	38.2	28.2	30.9	36.2	42.1	19.1	26.4	29.6	42.4	20.6	29.0	18.1	40.7	18.0	35.1	40.2	3.9	41.7
Fe	27.0	16.3	28.2	20.6	22.8	4.7	18.0	13.5	7.01	3.0	29.9	19.9	17.0	1.3	26.3	18.2	30.3	0.9	27.3	12.9	1.4	93.5	0.6
O	47.2	53.9	46.5	51.9	49.0	55.5	52.4	54.2	55.7	54.7	49.9	50.5	52.0	56.1	50.8	52.0	49.8	58.1	51.2	50.6	57.9	–	56.5
Mn + Mg	0.6	0.8	0.6	0.5	2.5	–	1.2	1.0	0.1	0.1	0.9	2.9	0.9	0.1	1.6	0.3	0.8	–	0.8	0.2	0.1	2.6	–

than the Ti-rich areas. The chemical composition of different areas within the particles was analyzed employing the Energy-Dispersive Spectrometry (EDS). The measured values are provided in Table 2, and the corresponding phase of each point is matched with the characterized phases of the XRD analysis.

3.2.1 Ilmenite Ore

The ore is mainly consisting of ilmenite and pseudorutile. Therefore the amount of A1 and B1 particles is significantly higher than the other types. The rest of the particles have different alteration degrees and usually consist of at least two of ilmenite, pseudorutile, and rutile phases. Hence, Fig. 2 (A1 to E1) can show the evolution of the transformation of grains from ilmenite to pseudorutile and rutile through the weathering phenomenon.

3.2.2 Oxidized Particles

As mentioned above, in the first stage of the ilmenite oxidation, rutile and hematite are formed. In the second stage, the rutile network is destroyed and reacts with hematite to form pseudobrookite [16]. Therefore, the oxidized ilmenite phase is in the form of a pseudobrookite matrix in which rutile is dispersed. This pattern is seen in A2 and C2, which indicates the presence of ilmenite in the original particles (A1 and C1). Distribution of Ti (in rutile) and Fe (in pseudobrookite) in A2 is illustrated by the EDS mapping given in Fig. 3, which agrees with the described phase distribution for the oxidized ilmenite.

During the first stage of the ilmenite oxidation, the chemical potential of the reaction as a driving force results in the outward diffusion of iron cations from the grain. Therefore, during oxidation of the particles with a significant amount of
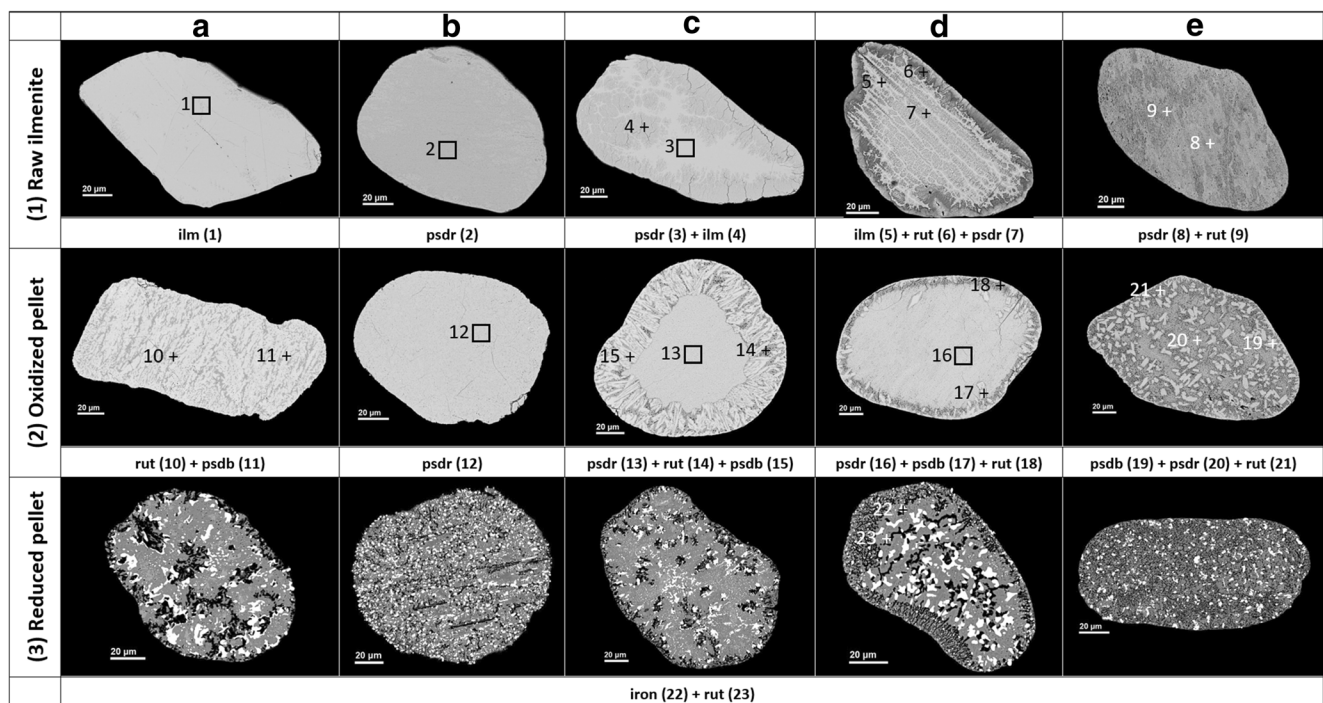

Fig. 2 The microstructure of different types of particles, **a–e**, in the altered ilmenite ore (1) and their possible corresponding particles after oxidation (2) and reduction (3). The mentioned phases below the particles' images are suggested based on the EDS and XRD analyses and the closest theoretical phase mentioned in the literature. (ilm: ilmenite; psdb: pseudobrookite; psdr: pseudorutile; rut: rutile)
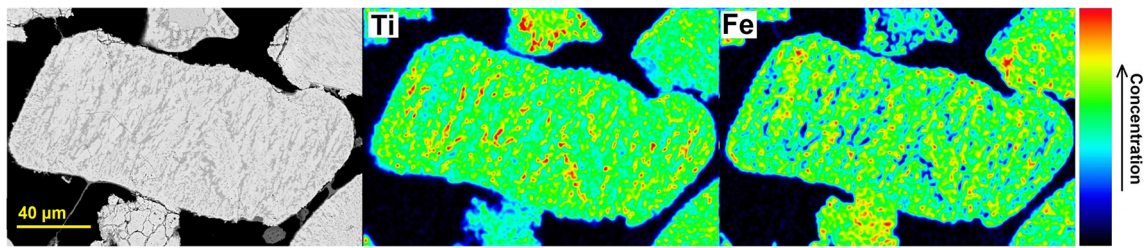
Fig. 3 EDS mapping of A2 particle (oxidized ilmenite). Distribution of Ti (rutile) and Fe (pseudobrookite)

ilmenite distributed close to the surface, a thin layer of hematite is usually formed at the edge. The thickness of this layer remains near 2 μm, and it may not grow further by increasing the oxidation time [16]. The microstructure of the oxidized pellet is shown in Fig. 4 in which a thin bright layer around the middle particle is observed. The EDS analysis of point 1 given in Fig. 4 confirms the formation of hematite on the particle's surface. In Fig. 2 this can be found in particles A2, C2, D2, and E2. However, due to a lower magnification, it cannot be recognized well.

With a big difference from the others, the pseudorutile phase remains relatively intact after oxidation. Comparison of B1 and B2 represents the phase transition of pseudorutile-based particles before and after oxidation, respectively. This morphology is identical in almost all the other particles that pseudorutile exists in. The presence of micropores and microcracks resulting from severe oxidation conditions are the characteristic features of the areas within the oxidized particles in which pseudorutile is the main phase present. An increased porosity in the oxidized particles was also observed in all the zones in which rutile exists. During the weathering of the starting ore, the formation of pseudorutile causes a 6% volume reduction, which leads to the formation of microcracks and porosities. The partially altered particles of C1 and D1 usually consist of a combination of pseudorutile, ilmenite, and rutile. Therefore, after the oxidation of such particles, in addition to increasing the porosity and formation of microcracks, rutile, pseudorutile, and pseudobrookite can be identified as dominant phases with different fractions. Studying the element mappings and chemical analysis of different areas in D1 and D2 demonstrates the effect of partial weathering on the phase distribution before and after oxidation. As can be seen in Fig. 5, the outer layer of D1 is rich with rutile. However, towards the core of the particles, pseudorutile and ilmenite are intergrown. Therefore, after the oxidation, as it is in D2, in addition to rutile, pseudorutile and pseudobrookite are the main constituent phases. The figure shows the isolation of ilmenite and pseudorutile (Fe-rich) in particle (a), and pseudobrookite and pseudorutile (Fe-rich) in particle (b) by a superficial rutile layer (Ti-rich).

Almost fully altered ilmenite particles are rutile-based with the typical morphology of E1. This type of particle has a

minority among the others with a dark gray BSE level. They contain ilmenite and pseudorutile in the minority that undergoes oxidation after the firing step, like what was stated about the other particle types.

3.2.3 Reduced Particles

The constituent phases of the reduced particles in most of the cases are identical. EDS analysis implies that a titanium (III) oxide matrix with dispersed reduced iron granules is the typical morphology of the reduced particles. However, depending on the phase distribution in the original particle, the phase distribution in the reduced particle varies. As is reported [15], the reduced iron grains of the highly altered particles are relatively finer than iron grains with pseudobrookite origin. This is well shown in Fig. 2 as B3 and E3 particles with fine iron grains spread in porous titanium (III) oxide matrix. The reason for this phenomenon is that the porosities in the oxidized pseudorutile provide nucleation sites for metallic iron during reduction. However, due to the presence of titanium oxide and pores, the opportunity for coalescence is low. Therefore, a lot of fine iron globules are formed in the highly altered particles. EDS elemental mapping of the reduced particles provided information about the concentration of Mg and Mn in some areas of the reduced particles. BSE micrographs of two different portions of reduced particles are given in Fig. 6, in which Figure 6 a shows the Mn-rich zones (light gray), and in Fig. 6b, the Mg-rich zones (dark gray) are seen. The EDS
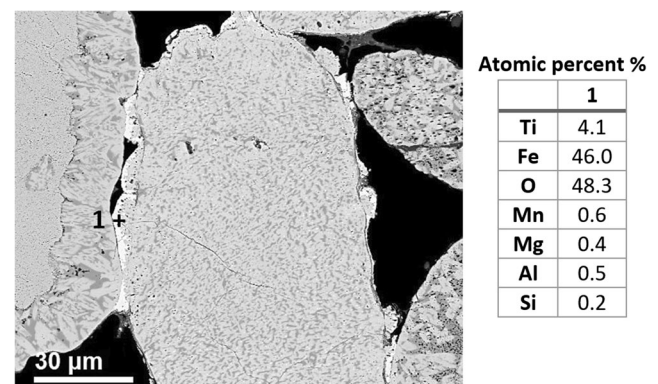

	Atomic percent %
	1
Ti	4.1
Fe	46.0
O	48.3
Mn	0.6
Mg	0.4
Al	0.5
Si	0.2

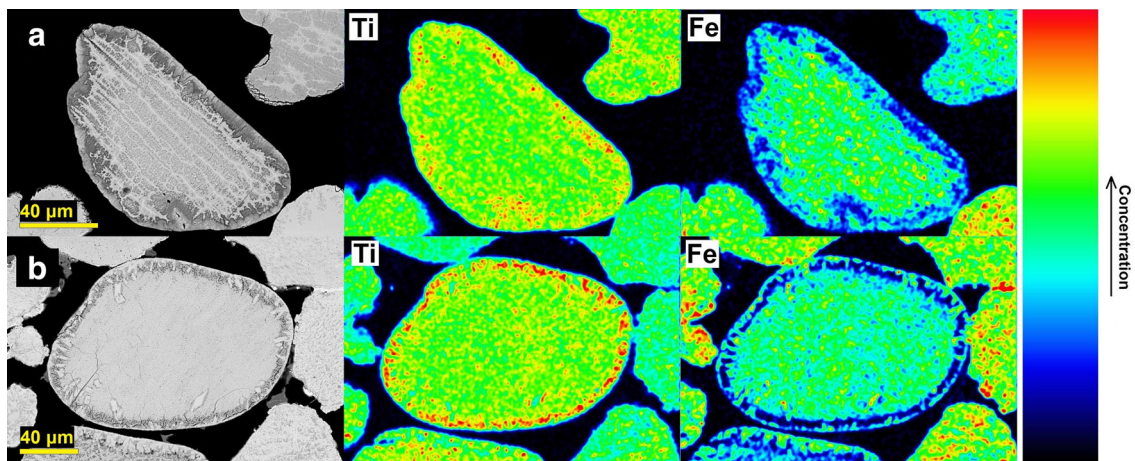**Fig. 4** Formation of a thin hematite layer on the surface of the oxidized particle

Fig. 5 Comparison of the EDS mapping of (**a**) D1 and (**b**) D2 particles (partially altered ilmenite before and after oxidation)

spectrums of points 1 and 2 and their corresponding chemical analysis are also given in the figure.

The chemical analysis of points 1 and 2 in Fig. 6 represents the apparent compounds of $Mn_2Ti_3O_5$ and $Mg_2Ti_3O_5$ in the reduced particles. The presence of the mentioned compounds agrees with the replacement of Mn and Mg in the ilmenite crystal structure. Considering the uncertainty of the EDS method and inhomogeneous phase distribution within the particles, the closest theoretical phases to points 1 and 2 are manganese α-oxide and armalcolite, respectively.

4 Conclusions

- In this study, phase transitions, microstructural changes, and element distribution of a weathered ilmenite concentrate were investigated using XRD and SEM techniques. From the obtained results, the following conclusions were drawn.

- Ilmenite, pseudorutile, and rutile are the main phases detected in the weathered ilmenite ore sample, and depending on the degree of weathering, different fractions of the phases were characterized in the ore particles.

- Oxidation of ilmenite to pseudobrookite consists of two main stages. In the first stage, rutile and hematite are formed, and by a combination of them in the second stage, a rutile phase dispersed in a pseudobrookite matrix is produced.

- No phase transition was detected for the pseudorutile phase in oxidation, and the morphological changes as the formation of microcracks and micropores were the sole change of the phase after the oxidation step. During the first stage of the oxidation of ilmenite grains, the chemical potential of the reaction as a driving force leads to an outward diffusion of iron towards the grain's surface. Therefore, at the edge of the particles with a significant amount of ilmenite distributed close to the surface, a thin layer of hematite is usually formed after oxidation.
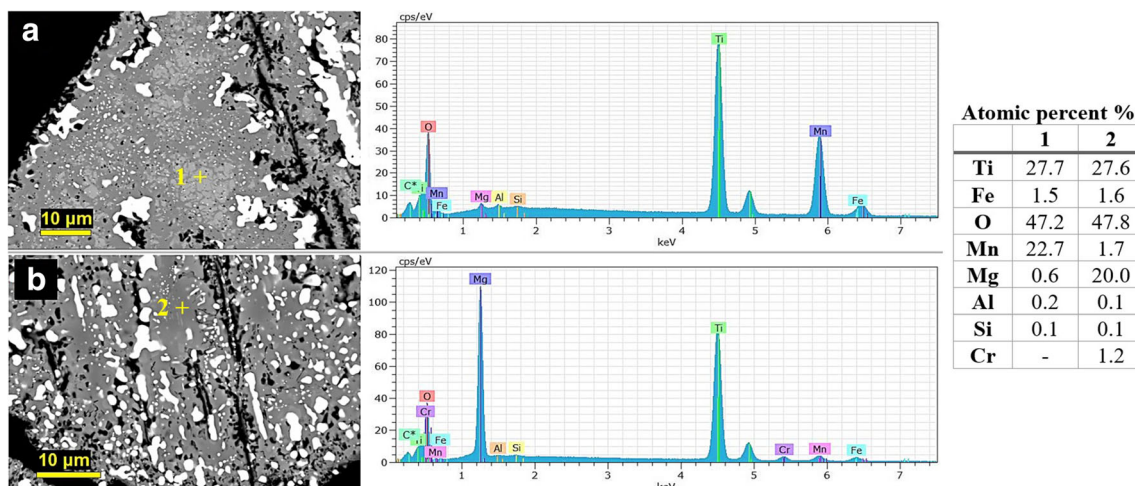

Atomic percent %		
	1	2
Ti	27.7	27.6
Fe	1.5	1.6
O	47.2	47.8
Mn	22.7	1.7
Mg	0.6	20.0
Al	0.2	0.1
Si	0.1	0.1
Cr	-	1.2

Fig. 6 Mn and Mg concentration in the reduced ilmenite as (**a**) manganese titanate (light gray) and (**b**) magnesium titanate (dark gray). On the right side, the EDS spectrum and chemical analysis of points 1 and 2 are given

- A titanium (III) oxide matrix with dispersed reduced iron granules is the typical morphology of the reduced particles. Although, depending on the alteration degree of the original particle, the morphology of the metallic iron grains varies from coarse in the poorly altered degree to fine in highly altered ones due to the higher porosity of the highly altered particles.
- The concentration of Mg and Mn in some of the particles indicates replacement of iron by these elements in ilmenite crystal structure during reduction.

Declarations

Conflict of Interest The authors declare no competing interests.

References

1. Lütjering G, Williams JC (2007) Titanium. Springer-Verlag, Berlin Heidelberg. https://doi.org/10.1007/978-3-540-73036-1
2. Habashi F (1997) Handbook of extractive metallurgy, Primary metals, secondary metals, light metals, vol 2. Wiley-VCH
3. Woodruff LG, Bedinger GM, Piatak NM (2017) Titanium. US Geological Survey. https://doi.org/10.3133/pp1802T
4. Elstad H, Seim S (2013) Titanium. In: Tangstad M (ed) Metal production in Norway. Akademika forlag, Trondheim
5. Pan RJ, Yang SL (2013) Comparison of one-step method and two-step method of ilmenite concentrate smelting titanium slag. Adv Mater Res 704:77–86. https://doi.org/10.4028/www.scientific.net/AMR.704.77
6. Zhang Y, Zhao J, Ma X, Li M, Lv Y, Gao X (2019) Isothermal reduction kinetics and mechanism of pre-oxidized ilmenite. Min Metall Explor 1–13
7. Lv W, Lv X, Lv X, Xiang J, Bai C, Song B (2018) Non-isothermal kinetic studies on the carbothermic reduction of Panzhihua ilmenite concentrate. Miner Process Ext Metall 1–9
8. Salehi H, Aghajani H, Salimkhani H (2018) Isothermal and kinetic studies on oxidation roasting of Kahnooj ilmenite concentrate. Chem Eng Trans 66:397–402. https://doi.org/10.3303/CET1866067
9. Mozammel M, Sadrnezhaad SK, Khoshnevisan A, Youzbashizadeh H (2012) Kinetics and reaction mechanism of isothermal oxidation of Iranian ilmenite concentrate powder. J Therm Anal Calorim 112(2):781–789. https://doi.org/10.1007/s10973-012-2639-1
10. Gou HP, Zhang GH, Chou KC (2015) Influence of pre-oxidation on carbothermic reduction process of ilmenite concentrate. ISIJ Int 55(5):928–933. https://doi.org/10.2355/isijinternational.55.928
11. Lobo S, Kolbeinsen L, Seim S (2016) Reduction of Norwegian and Indian ilmenite with carbon monoxide and hydrogen gas blends. Can Metall Q 55(4):455–462. https://doi.org/10.1080/00084433.2016.1206291
12. Merk R, Pickles C (1988) Reduction of ilmenite by carbon monoxide. Can Metall Q 27(3):179–185
13. Grey IE, Reid AF (1975) The structure of pseudorutile and its role in the natural alteration of ilmenite. Am Miner: J Earth Planet Mater 60(9-10):898–906
14. Mücke A, Chaudhuri JB (1991) The continuous alteration of ilmenite through pseudorutile to leucoxene. Ore Geol Rev 6(1):25–44
15. Gupta SK, Rajakumar V, Grieveson P (1989) The influence of weathering on the reduction of llmenite with carbon. Metall Trans B 20(5):735–745
16. Zhang JB, Zhu QS, Xie ZH, Lei C, Li HZ (2013) Morphological changes of Panzhihua ilmenite during oxidation treatment. Metall Mater Trans B Process Metall Mater Process Sci 44(4):897–905. https://doi.org/10.1007/s11663-013-9863-3
17. Dewan MA, Zhang G, Ostrovski O (2010) Carbothermal reduction of a primary ilmenite concentrate in different gas atmospheres. Metall Mater Trans B 41(1):182–192

Publisher's Note Springer Nature remains neutral with regard to jurisdictional claims in published maps and institutional affiliations.